Electron Cloud Density Generated by Microring-Embedded Nano-grating System

M. Bunruangses, P. Youplao, I. S. Amiri, N. Pornsuwancharoen, S. Punthawanunt, G. Singh & P. Yupapin

Plasmonics

ISSN 1557-1955

Plasmonics
DOI 10.1007/s11468-019-01083-9

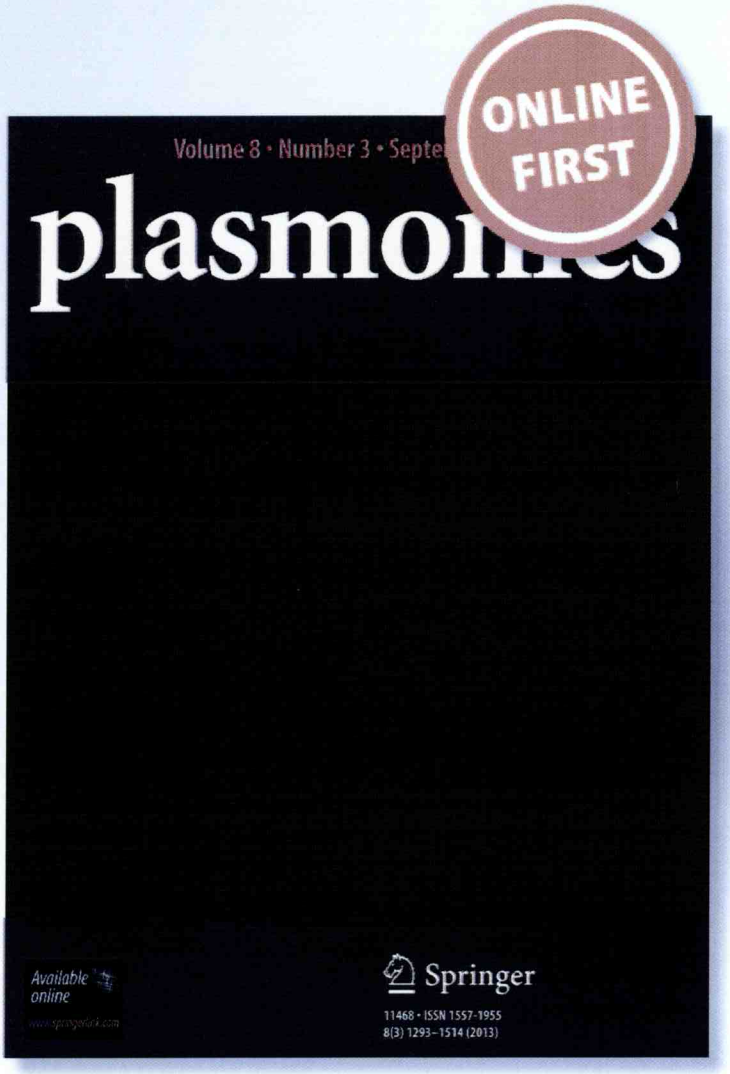

Springer

Plasmonics
https://doi.org/10.1007/s11468-019-01083-9

Electron Cloud Density Generated by Microring-Embedded Nano-grating System

M. Bunruangses[1] · P. Youplao[2] · I. S. Amiri[3] · N. Pornsuwancharoen[2] · S. Punthawanunt[4] · G. Singh[5] · P. Yupapin[3,6]

Received: 12 August 2019 / Accepted: 11 November 2019

Abstract
We propose the use of the electron cloud generated by quasi-particle waves called polariton dipoles, which oscillated within a silicon microring-embedded gold grating system for quantum consciousness processing model. An embedded gold grating is coupled by a whispering gallery mode beam generated by a soliton pulse, from which the polariton waves oscillated with the plasma frequency at the Bragg wavelength. The excited polariton cloud by the external stimuli can be detected at the system output ports. The two states of the polariton (electron) are spin-up and spin-down that can process automatically and deliver to the network and cloud. In manipulation, the results obtained show the electron density increased by increasing the input power into the system. In application, the cell polariton cloud coupled by the external stimuli and patterned by the quantum cellular automata results, which localized in the cloud network and connected to the nerve cell access nodes. The coded polaritons connected to the nerve cell memory clouds, while the required commands are delivered to resonant cells via the network link. More stenographic codes can also be generated by other external stimuli sources, which can process similarly.

Keywords Electron cloud source · High-density qubits · Quantum cellular automata · Quantum signal processing

Introduction

Origin of species was established by Darwin in 1859 [1, 2], where a century later, the greatest scientist Schrodinger raised the question "What is life?" in 1944 [3]. From which, scientists are still searching for the more clearly accommodated origin of life. One of the most closely related to Schrodinger postulation explained that the origin of life was formed by the coupling between the strong field and ionic dipole [4], where life began. In this concept, a tiny unit of life formed by the quasi-particle known as a polariton, which can propagate and link to the body and brain network via the liquid core waveguide and cell electron cloud. However, until date, there is no clear concept of quantum consciousness yet. Life cells having the negative and positive ions (electrical charges) when they are coupled by the strong electromagnetic field [5–7] can generate the ionic dipole

✉ P. Yupapin
preecha.yupapin@tdtu.edu.vn

M. Bunruangses
montree.b@rmutp.ac.th

P. Youplao
phichai.yo@rmuti.ac.th

I. S. Amiri
irajsadeghamiri@tdtu.edu.vn

N. Pornsuwancharoen
nithiroth.po@rmuti.ac.th

S. Punthawanunt
suphanchai.pun@kbu.ac.th

G. Singh
gsingh.ece@mnit.ac.in

[1] Department of Computer Engineering, Faculty of Industrial Education, Rajamangala University of Technology Phra Nakhon, Bangkok 10300, Thailand

[2] Department of Electrical Engineering, Faculty of Industry and Technology, Rajamangala University of Technology Isan, Sakon Nakhon Campus, Sakon Nakhon 47160, Thailand

[3] Computational Optics Research Group, Advanced Institute of Materials Science, Ton Duc Thang University, District 7, Ho Chi Minh City, Vietnam

[4] Multidisciplinary Research Center, Faculty of Science and Technology, Kasem Bundit University, Bangkok 10250, Thailand

[5] Department of ECE, Malaviya National Institute of Technology Jaipur (MNIT), Jaipur, India

[6] Faculty of Applied Sciences, Ton Duc Thang University, District 7, Ho Chi Minh City, Vietnam

Published online: 22 November 2019

and be oscillated by the plasma frequency (ω_p), which is presented by the electron cloud distribution. The electron density of the cloud is n [8–10], from which the spins of the electron cloud are affected by the external environment (stimuli) and the quantum bits are processed by the quantum cellular automata (QCA) method [10, 11], where the final cloud spin states will transmit to the cloud network. The quantum consciousness is formed by the set of quantum codes from the quantum cellular automata, which communicated in human society. The finalized codes are delivered to the network and cells, where the resonant organs (parts) will function through a different organ mechanism. The resonant frequency is described by the time function, while the cell and organ natural frequency are the plasma frequency formed by the space function. The resonant human time function frequency is higher than an animal. Therefore, an animal cannot process the quantum cellular automata codes, which is affected and submerged in the noise floor. We assumed that human life is formed by the coupling between the strong electromagnetic field and ionic dipoles, which become fertilized sperm and egg in the ovum. The moving sperm introduces the shock wave which is the space function called a soliton before fertilizing the egg. There are the positive and negative ions in the egg. In principle, life is formed by the coupling between the strong fields and the ionic dipoles. The ionic dipoles are formed by the soliton pulse coupled to ion cloud. The time function formed by the Schrodinger time function is a wave-particle duality aspect. It is traveling via the time tunnel to generate the resonant frequency to the life cells. The photon transfers to the electron cloud, where the quantum consciousness is established by the quantum coding/decoding method called quantum cellular automata (QCA). The spiritual transmission line is formed and the certain form and frequency band of life have begun. In this article, we combined the Schrodinger wave-particle aspect with the time function and the ionic dipole oscillation of Bohm theory by the space function together [5–7]. The plasma frequency of the quasi-particle (polariton) oscillation is identified by the Bragg wavelength output peak intensity, from which the electron density is obtained, which is related to the quantum bit forming by the quantum cellular automata processing. Till date, the electron cloud can be generated by the various forms [11–14]. But in this proposal, the electron cloud can be generated by the Drude model [8–10], where the change in the input power can form the quantum codes by time-function switching, which is the quantum cellular automata. Regarding the Bohm theory, human cells are surrounded by the electron cloud around the nucleus, where the wave particles form called a polariton [4–7]. The motivation of the proposed device (circuit) is that it can generate the polariton wave [15], which can couple to the electron cloud and human cells, which allowed cell and brain communication [16, 17]. From which, the use of the circuit for brain interfacing and robot-like human (humanoid robot) may be possible. The experiment can be performed by applying the other coupling electron cloud sources, from which the communication between them is detected. The applied simulation programs are the Opti-wave and MATLAB programs; the related theory is given. Results of the simulation are discussed.

Theoretical Background

The coupling between the strong fields and the ionic dipoles from egg can form life, where the space-function is established. The time function from the time tunnel in space is projected instantly, and the origin of human life began. However, there are some cases that life can be formed without the time-function for the origin of life. The quantum consciousness is operated by the spin coding of the electron cloud, which is called the quantum cellular automata, which can be integrated and described by the following details.

The space-function of one dimension is given by a soliton pulse in the z-direction as [18, 19]

$$\mathrm{S}(\mathrm{z},\mathrm{t}) = \boldsymbol{A}\mathbf{sech}\left[\frac{\boldsymbol{T}}{\boldsymbol{T_0}}\right]\left[e^{\left[\frac{z}{2L_D}\right]}\right] \tag{1}$$

The phase term and soliton pulse dispersion in the waveguide are neglected because they are included in the simulation, where other soliton parameters are found in the provided reference [21]. The propagation distance is demonstrated by z. The propagation time for soliton pulse moving with a group velocity in a frame is $T = t - \beta_1 \times z$. Here, ω_0 is the frequency shift of the soliton.$L_d = T_0^2/|\beta_2|$ represents the dispersion length of the soliton pulse, where T_0 shows the soliton pulse propagation time at the initial input. The coefficients of the linear and the second-order terms of Taylor's expansion of the propagation constant are β_1 and β_2, respectively. For the soliton pulse in the microring device, a balance should be achieved between the dispersion length (L_d) and the nonlinear length $L_{NL} = 1/\Gamma\varphi_{NL}$, where $\Gamma = n_2K_0$ is the length scale over which is dispersive. For a soliton pulse, there is a balance between dispersion and nonlinear lengths; hence, $L_d = L_{NL}$. However, in this work, all parameters are obtained from the graphical method, and they are applied and confirmed by the MATLAB program.

The Drude model of the plasma wave frequency induced by the plasmonic wave on the metal surface has the relationship to change between plasma wave frequency and electrical power, where in this case, transducer mechanism can be described by the following [8–10].

$$\epsilon(\omega) = 1 - \frac{\mathbf{ne^2}}{\epsilon_0 \mathbf{m}\omega^2} \tag{2}$$

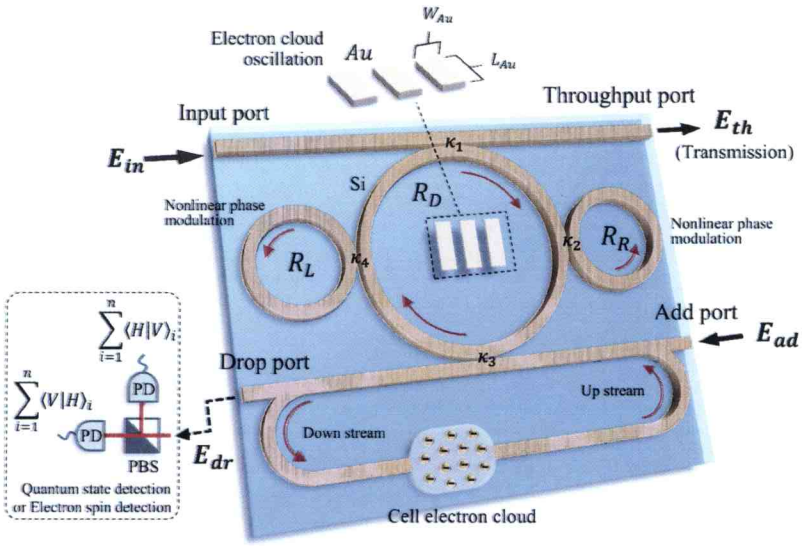

Fig. 1 The proposed microring circuit, where R_D, R_L, and R_R are the radii of the centre, the left, and the right ring, respectively. κ_s are the coupling coefficients. E_{in}, E_{th}, E_{ad}, and E_{dr} represent the electrical fields each at the input port, throughput port, add port, and drop port, respectively. The isolator and reflector are applied to protect the feedback and filtering purpose. <H and V> are the horizontal and vertical polarization components

where ϵ_0 is the relative permittivity;n, e, and m are the electron density, charge, and mass, respectively. ω is the angular frequency. The resonant frequency (ω_p) is called the plasma frequency.

The dielectric function changes the sign from negative to positive and real part of the dielectric function to zero, where the plasma resonant frequency is expressed by

$$\omega_p = \left[\frac{ne^2}{\epsilon_0 m}\right]^{1/2} \tag{3}$$

From the equation, the electron density is $n=\frac{\omega_p^2 \epsilon_0 m}{e^2}$. The plasmonic wave oscillation obtained by using an electric field is the longitudinal wave oscillation. By using the Maxwell equations, the TM polarization and exponential decay of the electric field are obtained. The input light source to the gold grating wavelength is λ. The resonant wavelength is related to the Bragg wavelength and is given by $\lambda_B = 2n_e\wedge$, where n_e is the effective refractive index of the grating in the waveguide, and $\wedge$ is the grating period.

The time function is by the photon energy oscillation given by

$$\mathbf{B}.e^{-i\omega_2 t_2} \tag{4}$$

where $\omega_2 t_2 = 2\pi\gamma_2 t_2$. ω_2, γ_2, and t_2 are the angular, linear frequency, and time, respectively. B is a constant. The four-wave mixing introduced by a nonlinear effect known as the Kerr effect is given by the relationship as $n = n_0 + n_2 I = n_0 + n_2 P/A_{eff}$, where n_0 and n_2 are the linear and nonlinear refractive indices, respectively. I is the

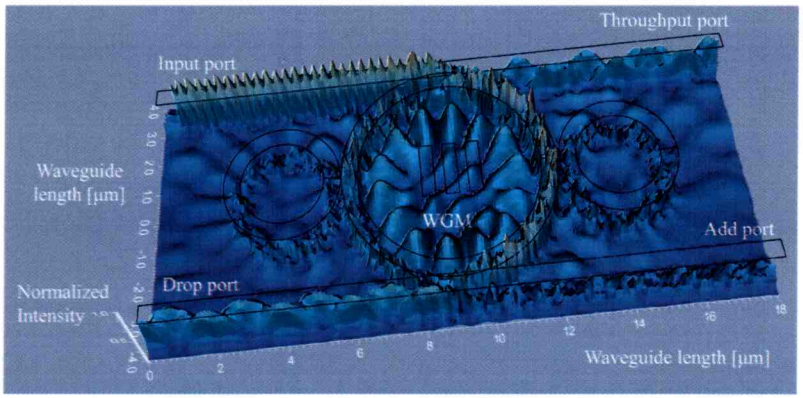

Fig. 2 Graphical results obtained by the Opti-wave program, where R_D = 3.0 μm, $R_L = R_R$ = 1.5 μm, each κ = 0.5, input = 100 mW, add = 100 mW, with the center wavelength of 1.55 μm and 1.30 μm, respectively. The gold gratings are detailed as W_{Au}= 0.4 μm, L_{Au}= 1.6 μm, with the grating periods of 0.3 μm and placed at 0.50 μm high above the lower cladding base. The waveguide loss is 0.1 dBmm^{-1}, and the effective core area is 0.25 μm^2. The refractive indexes of *Si* are $n_{1(Si)}$= 3.47 and $n_{2(Si)}$= 4.47 × 10^{-18} m^{2}W^{-1} [20]

Table 1 The selected parameters of the system for manipulation

Parameters	Symbols	Values	Units
Optical centre wavelength	λ	1.30, 1.55	μm
Radii of the ring resonator	R_s	1.5–3.0	μm
Coupling coefficient	κ	0.5	-
Waveguide loss	α	0.1	dB $(mm)^{-1}$
Waveguide core effective area	A_{eff}	0.25	μm^2
Gold grating width	W_{Au}	0.4	μm
Gold grating length	L_{Au}	1.6	μm
Gold grating thickness	-	0.2	μm
Grating period	Λ	0.7	μm
Plasma frequency	ω_p	-	$rads^{-1}$
Electron density	n	-	Electrons m^{-3}
Permittivity of free space	ϵ_0	8.85×10^{-12}	F m^{-1}
Electron mass	m	$9.11 \times 10^{-11}10$	kg
Electron charge	e	1.6×10^{-19}	Coulomb
Waveguide's 2refractive index	$n_{1(Si)}$	3.47	-
	$n_{2(Si)}$	4.47×10^{-18}	m^2W^{-1}

optical intensity and P is the optical power, where A_{eff} is the effective mode core area of the device. For the microring resonator, most of the effective mode core areas range from 0.1 to 0.50 μm^2.

The transmission formed by the unified space-time function is given by

$$\psi(z, t) = \bar{A}\ \mathbf{sech}\left[\frac{T}{T_0}\right]\left[e^{\left[\frac{Z}{2L_D} - i(\varphi_1+\varphi_2)t\right]}\right] = Ae^{-i(\varphi_1+\frac{E_n}{n\hbar})t} \quad (5)$$

where $A=\bar{A}\ \mathbf{sech}\left[\frac{T}{T_0}\right]\mathbf{exp}(\frac{Z}{2L_D})$, $\boldsymbol{\varphi_1 = 2\pi\gamma_1 t}$ is the phase of the time multiplexing function. $\boldsymbol{\varphi_2(t)}=\frac{E_n}{n\hbar}$, $\boldsymbol{\omega_2 = 2\pi\gamma_2 = \frac{E_n}{n\hbar}}$ = nhv; n = 1, 2, 3... It is a synchronous multiplexing scheme. The input sources are simultaneously fed into the system; the time (t) is the same. The transmission output can be detected at the system ports and the WGM outputs, which can be applied to the downstream side as well. The optical filter and de-multiplexer are applied. The quantum bits detection can be applied in both methods in either spin- or polarized-oriented detections as shown in Fig. 1. The set of quantum bits is processed by the quantum cellular automata processing and is transferred to the electron cloud.

Simulation Results

The space function is a soliton pulse, fed into the system to excite the gold grating, from which the plasmonic wave and polariton dipoles are oscillated at the Bragg wavelength. The

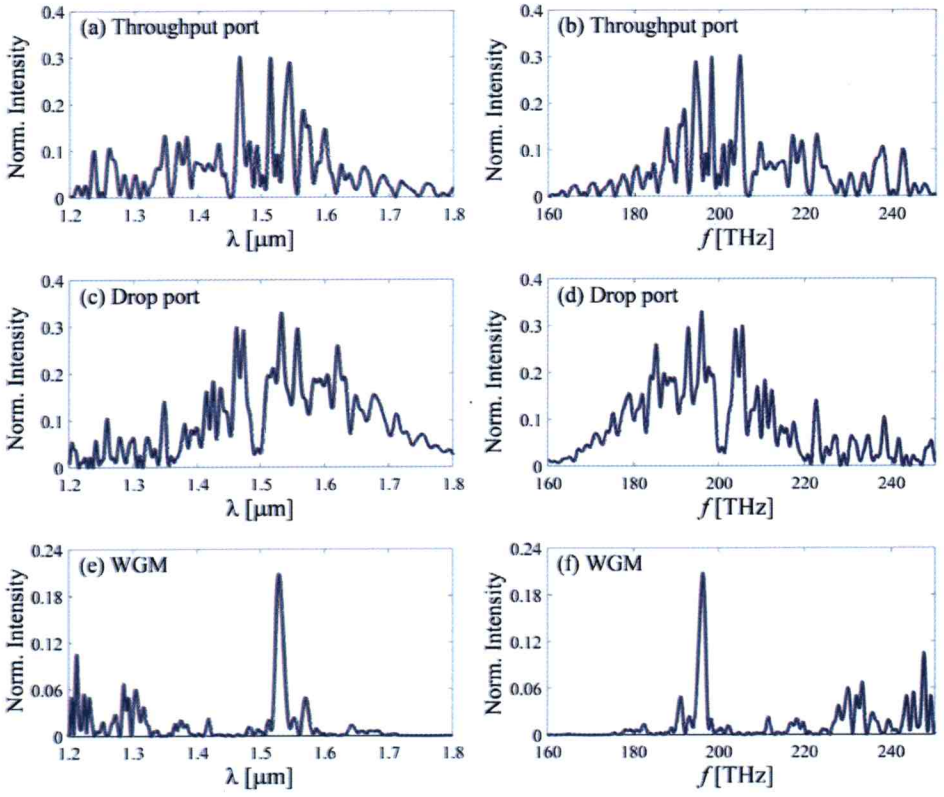

Fig. 3 The plot of obtained signals with wavelength and frequency, where (**a**) and (**b**) are the throughput port signals, (**c**) and (**d**) drop port signals, and (**e**) and (**f**) WGM signals. The output wavelength shifted from 1.55 μm due to the Bragg wavelength applied

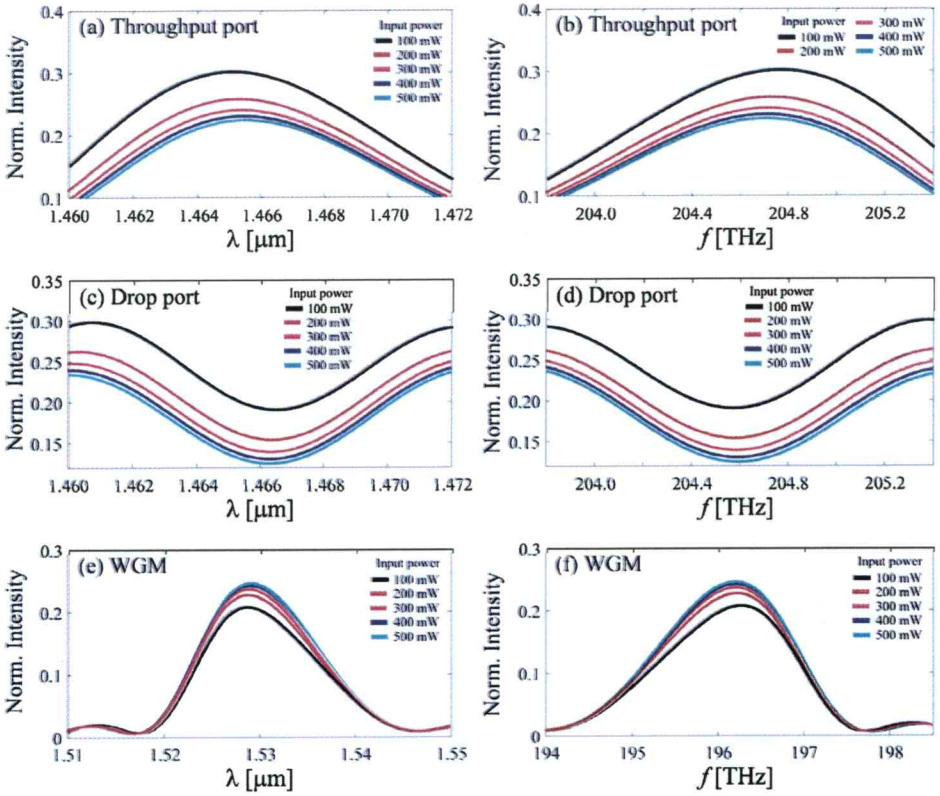

Fig. 4 The plot of the obtained signals by varied input port power from 100 to 500 mW, where (**a**) and (**b**) are the throughput port signals, (**c**) and (**d**) drop port signals, and (**e**) and (**f**) WGM signals, with wavelength and frequency. The output wavelength shifted from 1.55 μm due to the Bragg wavelength applied

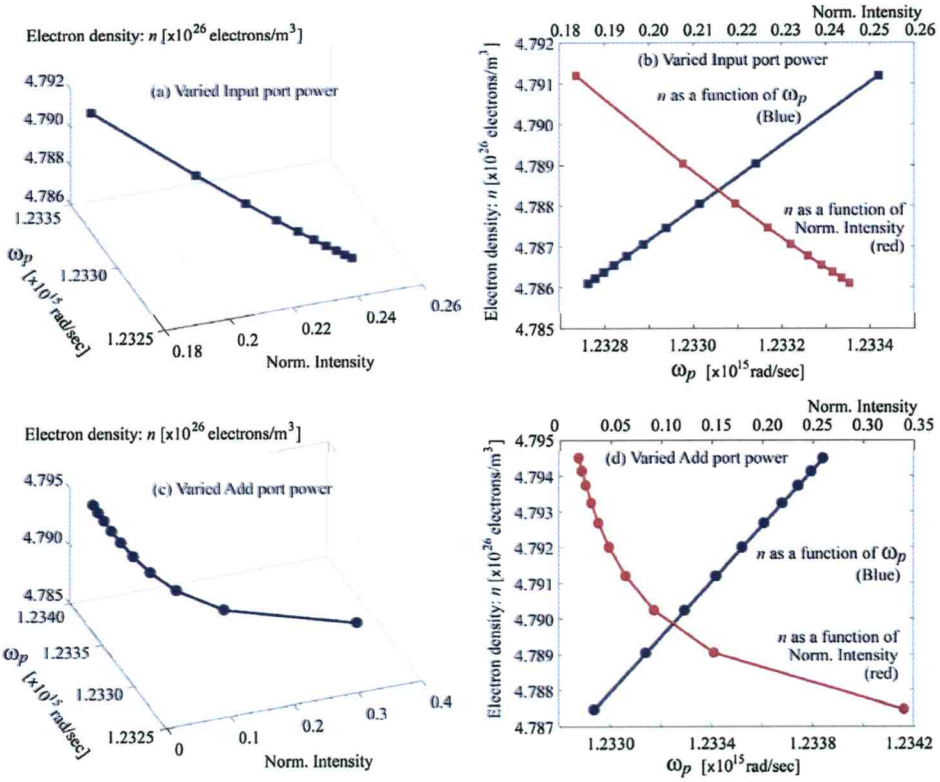

Fig. 5 The plot of the MATLAB program results of the normalized output and the electron density $\left[n = \frac{\omega_p^2 \epsilon_0 m}{e^2}\right]$, where (**a**) and (**b**) are varied input port power and fixed add port power, (**c**) and (**d**) fixed input port power and varied add port power. The change in the input power of the system (chip) can change the electron density, which means that the set of quantum bits of the quantum cellular automata changed and linked to the cloud network and cells

resonant signal reflected back to the system, while the whispering gallery mode (WGM) propagated and form the plasmonic antenna at the Bragg wavelength. By using the suitable parameters, the WGM beam is generated and coupled with the grating; the dipole oscillation of the quasi particles called polariton is generated, which is the plasma wave with the specified Bragg wavelength and plasma frequency. The time function is applied simultaneously (synchronously) via the add port; however, the different time functions can be applied to have more packets of waves to form the asynchronous and stenographic applications. The clock generated by the soliton pulse can address the transmission bits. The polariton spin-up and spin-down will be used to form the memory code for each packet of signals; eventually, the stenographic codes are recognized and existed in the cloud. By using the system in Fig. 1, the manipulation of the electron cloud density is shown in Fig. 2. The selected parameters are given in Table 1. The graphical results are obtained by the Opti-wave program and the required whispering gallery mode is obtained, which formed to drive the gold plate electrons. The main parameter of the system is the side ring radius, which can arrange to have the space uncertainty saturation, where the squeezing light (WGM) can be obtained. The plot of obtained signals of the system with wavelength and frequency is shown in Fig. 3, where the obtained signals by varying the input power from 100 to 500 mW are shown in Fig. 4. The plot of the MATLAB program results of the normalized output and the electron density $\left[\boldsymbol{n} = \frac{\omega_p^2 \epsilon_0 m}{e^2}\right]$ is shown in Fig. 5. Principally, the excited electron cloud within the system by the external stimuli will process the spin-up and spin-down automatically by the quantum cellular automata, from which the quantum codes are localized in the transmission cloud network. One of the applications is the use of the electron cloud system (chip) for humanoid brain processing, where the humanoid ethics can be implemented by the quantum bits, which are known as quantum consciousness. The humanoid brain needed the human-like brain function, where the quantum consciousness processing is an important part. The memory is formed by the time axis where it consists of the neutral point where there is no function, which is at rest position (neutral). The other two sides of the time axis are the positive and negative directions of the neutral position. The projection of the QCA codes can connect in any position on the time axis which is given by the time function, $e^{+i\omega t}$, e^{0}, and $e^{-i\omega t}$ where the QCA codes are processed by the time function to be the quantum consciousness. The communication between the generated codes and cell cloud is recognized and transmitted into the networks.

Conclusion

We demonstrated the use of unified space-time function control within the microring circuit for the electron cloud generation. The electron cloud is generated by the space-function (soliton pulse). The spin states are controlled by the time-function, which is classified by the time sequence. The electron spin state is transmitted via the polariton (electron spin wave), in which the communication network is established. Such result can offer the use for electron cloud spin coding called the quantum cellular automata (QCA), where the automatic coding of the electron cloud is established and transmitted by the spin waves. In application, various inputs (polaritons) can be processed and transmitted to link with the cell electron cloud, from which the electron spin information can connect the cells and transmit to the network. The projection of the spin states (quantum bits) can link to the nerve cells, while the spin codes localized are memorized in the transmission network. The results obtained have shown that the use of the QCA can be possible and be used to form like human quantum consciousness, which can be applied in the ethic robotic brain. Therefore, the use of the integrated circuits of the QCA chip has the potential for the ethic humanoid robot brain applications.

Acknowledgments The authors would like to acknowledge the research facilities from Ton Duc Thang University, Vietnam, and the financial support from Rajamangala University of Technology Phra Nakhon, Bangkok 10200, Thailand.

References

1. Clarson SJ (2009) Charles Darwin and silicon. Silicon 1:59–63
2. Oldroyd DR (1986) Charles Darwin's theory of evolution: a review of our present understanding. Biol Philos 1(2):133–168
3. Schrodinger E (1967) What is life ? The physical aspect of the living cells & mind and matter. Cambridge University Press, London
4. Poznanski RR, Cacha LA, Latif AZA, Salleh SH, Ali J, Yupapin P, Tuszynski JA, Tengku MA (2019) Theorizing how the brain encodes consciousness based on negentropic entanglement. J Integr Neurosci 18(1):1–10
5. Poznanski RR et al (2017) Solitonic conduction of electrotonic signals in neuronal branchlets with polarized microstructure. Sci Rep 7:2746
6. Bohm DJ (1952) A suggested interpretation of the quantum theory in terms of hidden variables. Phys Rev 85:166–193
7. Bohm DJ (1990) A new theory of the relationship of mind and matter. Philos Psychol 3:271–286
8. Robert LO et al (2012) Optical dielectric function of gold, Physical review, 2012. B 86(235147):1–9
9. Derkachova A, Kolwas K (2007) Size dependence of multipolar plasmon resonance frequencies and damping rates in simple metal spherical nanoparticles. Eur Phys J-Spec Top 144:93–99
10. Tunsiri S et al. (2019) Microring switching control using plasmonic ring resonator circuits for super-channel use, Plasmonics, First online 22: 1-9.

11. Awschalom DD et al (2018) Quantum technologies with optically interfaced solid-state spins. Nature Photonics 12:516–527
12. Herold M et al. (2015) Cellular-automation decodeers for topological quantum memories, NPJ Quantum Information: 1; Article number 15210
13. Gács P (2001) Reliable cellular automata with self-organization. J Stat Phys **103**:45–267
14. Aizatsky NI et al (2016) Generation and formation of axially symmetrical tubular electron beam in a cold metal secondary-emission cathode magnetron gun-part II: Computer modeling. IEEE Transaction on Electron Devices 63(4):1710–1714
15. Ali J et al (2018) Characteristics of an on-chip polariton successively filtered circuit. Results in Physics 11:410–413
16. Bunruangses M et al (2019) Brain sensor and communication model using plasmonic microring antenna network. Opt Quant Electron 51:349
17. Bunruangses M et al (2019) Microring distributed sensors using space-time function control. IEEE Sensors J:1–1. https://doi.org/10.1109/JSEN.2019.2945772
18. Agrawal GP (2011) Nonlinear fiber optics: its history and recent progress, [Invited]. J Opt Soc Am B 28(12):A1-A10
19. Phatharaworamet T et al (2010) Random binary code generation using dark-bright soliton conversion control within a panda ring resonator. IEEE Lightwave Technol 28(19):2804–2809
20. Yue Y et al (2012) Silicon-on-nitride waveguide with ultralow dispersion over an octave-spanning mid-infrared wavelength range. IEEE Photonics J 4(1):126–132